



Mitotic spindle formation in the absence of Polo kinase

Juyoung Kim^a and Gohta Goshima^{a,b,1}

Edited by Geert Kops, Hubrecht Institute, Utrecht, the Netherlands; received August 5, 2021; accepted February 2, 2022 by Editorial Board Member Rebecca Heald

Mitosis is a fundamental process in every eukaryote, in which chromosomes are segregated into two daughter cells by the action of the microtubule (MT)-based spindle. Despite this common principle, genes essential for mitosis are variable among organisms. This indicates that the loss of essential genes or bypass of essentiality (BOE) occurred multiple times during evolution. While many BOE relationships have been recently revealed experimentally, the bypass of essentiality of mitosis regulators (BOE-M) has been scarcely reported, and how this occurs remains largely unknown. Here, by mutagenesis and subsequent evolutionary repair experiments, we isolated viable fission yeast strains that lacked the entire coding region of Polo-like kinase (Plk), a versatile essential mitotic kinase. The BOE of Plk was enabled by specific mutations in the downstream machinery, including the MT-nucleating γ -tubulin complex, and more surprisingly, through down-regulation of glucose uptake, which is not readily connected to mitosis. The latter bypass was dependent on casein kinase I (CK1), which has not been considered as a major mitotic regulator. Our genetic and phenotypic data suggest that CK1 constitutes an alternative mechanism of MT nucleation, which is normally dominated by Plk. A similar relationship was observed in a human colon cancer cell line. Thus, our study shows that BOE-M can be achieved by simple genetic or environmental changes, consistent with the occurrence of BOE-M during evolution. Furthermore, the identification of BOE-M constitutes a powerful means to uncover a hitherto understudied mechanism driving mitosis and also hints at the limitations and solutions for selecting chemotherapeutic compounds targeting mitosis.

mitotic spindle | experimental evolution | *Schizosaccharomyces pombe* | microtubule nucleation | Polo-like kinase

Different organisms have different sets of essential genes for their viability and propagation (1, 2). This indicates that most “essential” genes are context dependent and can become dispensable during evolution. Plausibly, a loss of essentiality is compensated for by manifestation of an alternative, currently “masked,” or far less active mechanism to ensure a similar cellular activity. Many experimental efforts have been made to recapitulate the molecular diversity found in nature (3). Large-scale systematic surveys have been recently conducted in budding and fission yeasts, in which a number of bypass-of-essentiality (BOE) events have been identified (4–7). In these studies, suppressors were screened for haploid strains, in which an essential gene was experimentally disrupted. For 9 to 27% of the essential gene disruptants, a mutation or overexpression of other gene(s) or chromosomal gain makes the strain viable, indicating that essentiality depends on genetic background and that BOE could indeed occur at a certain frequency. However, in most cases, the underlying mechanism remains unexplored. It is also unclear why BOE is rarely observed in certain processes, such as mitotic cell division.

Mitotic cell division is controlled by many essential genes in a given cell type (8–10). Evolutionary evidence of BOE is clearly visible for this fundamentally critical biological process. One striking example is the centrosome, which is assembled by the action of many essential proteins in animal, fungal, and algal species and plays a vital role in cell division and cellular motility (11). However, the centrosome and most of its components have been lost in land plants, and yet, plant cells undergo spindle assembly and chromosome segregation at high fidelity (12). Kinetochores components, such as the Constitutive Centromere Associated Network (CCAN); spindle microtubule (MT)-associated proteins, such as TPX2, augmin, and mitotic motors; and cell cycle regulators, such as anaphase-promoting complex/cyclosome, are among other examples. They are not universally conserved or essential factors (12–15). Despite the evidence of BOE for almost all the genes involved in mitosis, only a limited number of cases can be found in experimental BOE screening. For example, two random BOE screenings in fission yeast encompassing 23 mitotic genes have identified only a single protein, Cnp20/CENP-T, despite the fact that >20% BOE has been observed for mitosis-unrelated genes (6, 7). The BOE of *cnp20* is conceivable, as CENP-T functions

Significance

Mitosis is an essential process in all eukaryotes, but paradoxically, genes required for mitosis vary among species. The essentiality of many mitotic genes was bypassed by activating alternative mechanisms during evolution. However, bypass events have rarely been recapitulated experimentally. Here, using the fission yeast *Schizosaccharomyces pombe*, the essentiality of a kinase (Plo1) required for bipolar spindle formation was bypassed by other mutations, many of which are associated with glucose metabolism. The Plo1 bypass by the reduction in glucose uptake was dependent on another kinase (casein kinase I), which potentiated spindle microtubule formation. This study illustrates a rare experimental bypass of essentiality for mitotic genes and provides insights into the molecular diversity of mitosis.

Author affiliations: ^aDivision of Biological Science, Graduate School of Science, Nagoya University, Nagoya 464-8602, Japan; and ^bSugashima Marine Biological Laboratory, Graduate School of Science, Nagoya University, Toba 517-0004, Japan

Author contributions: J.K. and G.G. designed research; J.K. and G.G. performed research; J.K. analyzed data; and J.K. and G.G. wrote the paper.

The authors declare no competing interest.

This article is a PNAS Direct Submission. G.K. is a guest editor invited by the Editorial Board.

Copyright © 2022 the Author(s). Published by PNAS. This open access article is distributed under Creative Commons Attribution-NonCommercial-NoDerivatives License 4.0 (CC BY-NC-ND).

¹To whom correspondence may be addressed. Email: goshima@bio.nagoya-u.ac.jp.

This article contains supporting information online at <http://www.pnas.org/lookup/suppl/doi:10.1073/pnas.2114429119/-/DCSupplemental>.

Published March 14, 2022.

in parallel with CENP-C for kinetochore assembly (16, 17). Another known bypass of essentiality of mitosis regulators (BOE-M) in fission yeast is MT plus end-directed kinesin-5/*Cut7*, which is required for bipolar spindle formation through force generation on spindle MTs. The viability of *cut7Δ* was restored when the opposing minus end-directed kinesin-14/*Pkl1* was simultaneously deleted. Thus, the balance of forces applied to spindle MTs is critical (18–20). However, many other essential mitotic genes have no apparent functionally redundant or counteracting factors, and whether these relationships are general mechanisms of BOE-M is unclear. Essential mitotic genes are potential targets of cancer chemotherapy (21); it is also important to understand the BOE that underlies drug resistance.

In this study, we found that the essentiality of the sole Polo-like kinase (Plk) in fission yeast (*Plo1*) can be bypassed. *Plo1*, similar to human *Plk1*, is assumed to be essential for spindle MT formation and spindle bipolarization. However, these essential processes were restored in the absence of *Plo1* by multiple independent mechanisms that increase MT nucleation and stabilization, one of which involved a remarkably simple change in glucose concentration in the culture medium and depended on casein kinase I (CK1). Thus, our study uncovered an unexpected alternative mechanism of spindle MT formation and further implies that more BOE-M can be recapitulated in the experimental system.

Results

Viable Yeast Cells without Plks in Several Genetic Backgrounds.

Our previous BOE screening randomly selected 93 genes on chromosome II, which encompassed 12 mitotic genes (7). BOE-M could not be detected in any of these genes. To further screen for BOE-M, we selected eight other mitotic genes (*ark1*, *bir1*, *fta2*, *fta3*, *mis6*, *mis14*, *pic1*, and *plo1*) and applied the same screening method. Seven days after plating and ultraviolet (UV) mutagenesis of spores of each disruptant, we found a growing haploid colony for *plo1Δ*, the sole Plk in *Schizosaccharomyces pombe* (Fig. 1A, first step). Plks play versatile roles in animal cell division, including centriole duplication (by *Plk4*), centrosome maturation, spindle assembly checkpoint satisfaction, and cytokinesis (by *Plk1*). It is also a possible target for cancer chemotherapy (21–23). The responsible suppressor mutation was identified through whole-genome sequencing (WGS) followed by genetic crossing, which turned out to be *glt5* (Fig. 1B, Left, fourth line). In *S. pombe*, eight hexose transporters have been identified, which show different affinities to glucose; *Ght5* is a major hexose transporter with the strongest affinity to glucose and plays a critical role in glucose uptake (24). This prompted us to test, and we found that the *plo1Δ* strain grows, albeit slower than the wild type, when the glucose concentration of the medium is lower than 0.3% (Fig. 1B, Left, third line and SI Appendix, Fig. S1A). Thus, *plo1Δ* became viable under low-glucose conditions. To obtain a full scope of suppressor mutations, we repeated the UV mutagenesis of *plo1Δ* spores on a larger scale, obtained multiple colonies, and determined the responsible mutations. Simultaneously, an “experimental evolution” [EVO; also called “evolutionary repair” (3)] experiment was conducted for the *plo1Δ* strain in low-glucose medium (0.08%), in which serial dilution and saturation enrich the cells that have acquired beneficial mutations for proliferation (Fig. 1A, “first EVO”). The faster-growing strains obtained through this step were subjected to further evolutionary repair

experiments in high-glucose medium (“second EVO”) and at a different temperature (“third EVO”).

We determined the WGS of several viable *plo1Δ* strains and confirmed the suppressor mutations by independently generating a double mutant with *plo1Δ*. In total, 16 genes were found to assist in the growth of the otherwise inviable *plo1Δ* strain (Fig. 1B and D and SI Appendix, Fig. S1B and C). An example of the evolutionary repair process is shown in SI Appendix, Fig. S1D. This strain acquired mutations in *alp6* and *aps1* during the first EVO but still possessed the benefit of the *plo1⁺* gene for strain fitness (SI Appendix, Fig. S1D, Left). However, additional mutations in *mip1* and *abh1* during the second EVO bypassed the requirement of *Plo1* since adding back the *plo1⁺* gene to the original locus did not further promote colony growth (SI Appendix, Fig. S1D, Right). Most of the responsible genes were categorized into three classes: the Spt-Ada-Gcn5 acetyltransferase (SAGA) complex, the glucose/protein kinase A (PKA) pathway, and MT regulators (Fig. 1D). The SAGA complex is a general regulator of transcription, possessing histone acetyltransferase activity, and affects the expression of many genes (25). We did not analyze this in the present study. The cyclic AMP (cAMP)/PKA pathway is linked to glucose homeostasis in fission yeast. Glucose is detected by a receptor (*Git3*), and the G-protein complex (*Gpa2*, *Git5*, and *Git11*) is activated, which then activates adenylate cyclase (*Cyr1*) to produce cAMP (26). Eventually, cAMP releases the inhibitor *Cgs1* from *Pka1*, converting *Pka1* to its active form (27). Furthermore, yeast cells regulate glucose uptake by changing the localization and transcriptional level of hexose transporters, including *Ght5*, depending on environmental conditions (24, 28, 29). There is a link between glucose/PKA and MT stabilizer cytoplasmic linker-associated protein during interphase (30). In our case, mutations in MT regulators (*alp4*, *alp6*, and *asp1*) and glucose/PKA pathway genes additively supported the growth of *plo1Δ* (Fig. 1B).

Monopolar Spindles Predominate during Mitosis in the Absence of Polo. The major MT nucleator at the centrosome is the γ -tubulin ring complex (γ -TuRC), which consists of γ -tubulin and gamma-tubulin complex protein (GCP) subunits, including GCP2 (*Alp4/Spc97*) and GCP3 (*Alp6/Spc98*) (31). In animal cells, *Plk1* is a critical regulator of mitosis, which is, in the early stage, required for γ -TuRC recruitment to the centrosome and thus, centrosome maturation; inhibition of *Plk1* leads to monopolar spindle formation (22, 32). In fission yeast, cytokinesis/septation defects are most profoundly observed in *plo1* mutants, whereas monopolar spindle formation has also been described (33–37). However, actual spindle dynamics have not been analyzed for *plo1Δ* in live imaging. To analyze spindle dynamics in the absence of *Plo1*, live imaging of mCherry-tubulin and a spindle pole body (SPB) marker, either *Sad1^{SUN}*-green fluorescent protein (GFP) or *Alp6^{GCP3}*-GFP, was performed after *plo1Δ* spore germination with spinning-disk confocal microscopy (Fig. 2A–E). The control cell assembled bipolar spindles immediately after the disappearance of interphase MT networks (Fig. 2A and D [time 0 corresponds to the onset of mitosis]), and cell division was completed in \sim 30 min. In contrast, 53 of 56 *plo1Δ* cells after spore germination were arrested with a monopolar spindle for >1 h (Fig. 2B, C, and E, wherein stronger laser exposure was applied in Fig. 2C to visualize the faint MT signals).

We compared the phenotype with other known mutants that show monopolar spindle formation, including *Cut12*, which drives SPB insertion into the nuclear envelope (NE) (38,

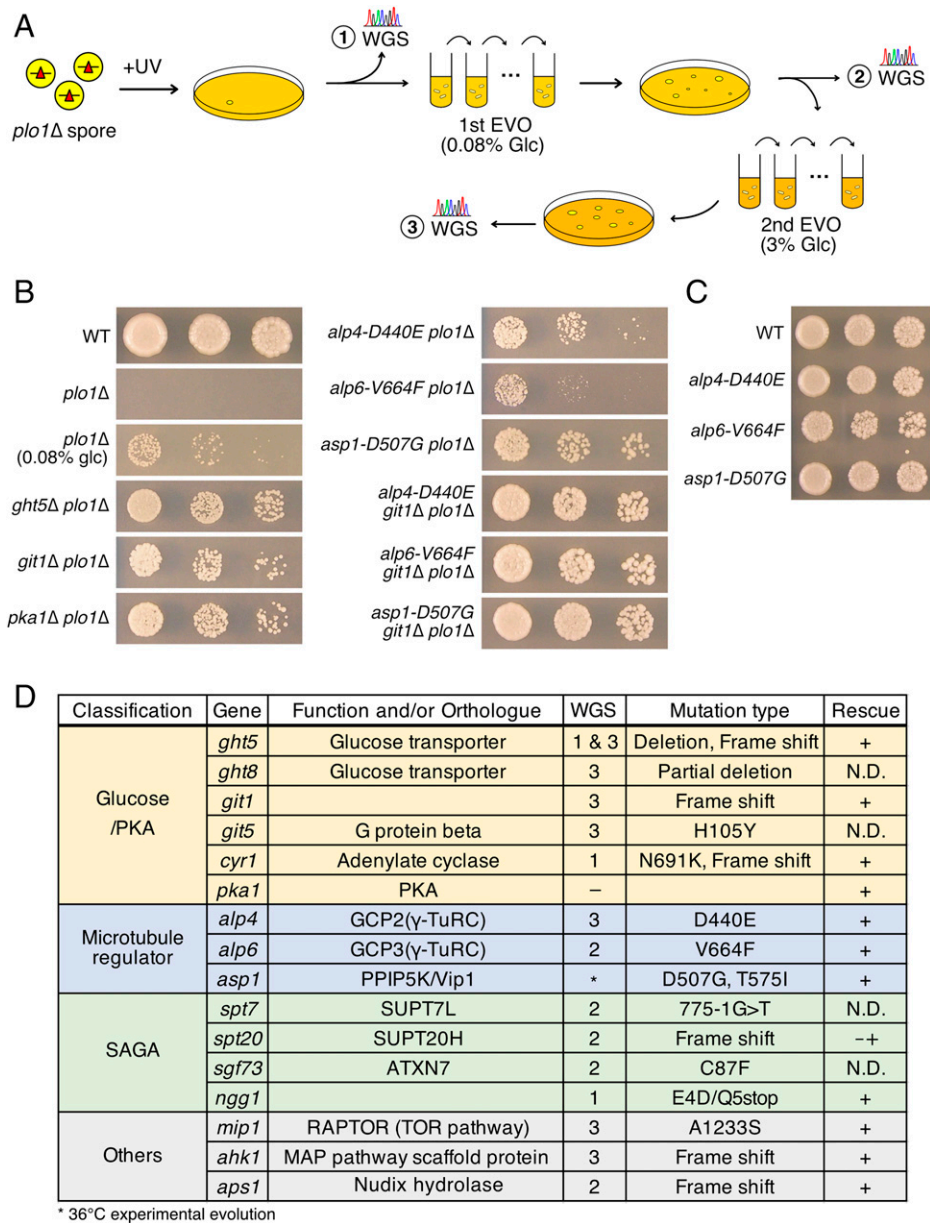


Fig. 1. Isolation of viable *plo1Δ* strains. (A) Experimental procedure to isolate *plo1Δ* strains. The yeast spores in which the *plo1* gene was replaced by drug-resistant cassette were mutagenized by UV and plated onto the drug-containing medium. The haploid colonies that appeared after several days represent the *plo1Δ* strains. The WGS was determined to map the responsible suppressor mutations, while a few strains were subjected to EVO, where serial dilution and saturation accumulated fitness-increasing mutations. EVO was repeated three times in different conditions, and suppressor mutations were determined by WGS. (B) Viable *plo1Δ* strains obtained by indicated suppressor mutations. Cells (5,000, 1,000, and 200) were spotted onto normal YE5S (yeast extract-based medium with five amino acid supplements) plates, except for in the third row, where glucose (glc) concentration in the medium was reduced to 0.08% (YE5S, 4 d, 32°C). (C) Single mutants of *alp4-D440E*, *alp6-V664F*, and *asp1-D507G*. Cells (5,000, 1,000, and 200) were spotted onto normal YE5S plates and incubated for 3 d at 32°C. (D) List of suppressor mutations for *plo1Δ*. The WGS column indicates at which step in A the mutation was identified. The rescue column indicates whether the indicated mutation alone bypassed the essentiality of *Plo1*. The colony grew extremely poorly for the *spt20Δ plo1Δ* (marked with –+). N.D., not determined; WT, wild type.

39); *Cut7^{kinesin-5}*, which is required for antiparallel MT cross-linking and sliding (40); and *Cdc31^{centrin}*, which is required for SPB duplication (41). In the *cut12-1* temperature-sensitive (ts) mutant, the lack of insertion of one of the duplicated SPBs causes partial breakage of the NE and detachment of an SPB from the NE (38, 42). In another study, *Plo1* was shown to regulate the formation of the *Sad1^{SUN}* ring structure, which might be required for SPB insertion (43). We assessed the integrity of the NE in *plo1Δ*. First, we tagged GFP to *Pcp1^{PCNT}*, a core SPB component (35, 44), in the *plo1Δ* background. In contrast to the *cut12-1* mutant, we always detected punctate *Pcp1^{PCNT}*-GFP signals ($n = 20$) at the pole of the monopolar spindle, suggesting

that SPBs in the NE generate spindle MTs in the absence of *Plo1* (SI Appendix, Fig. S2 A and B). Next, we conducted a nuclear localization signal (NLS)-GFP efflux assay, in which partial NE breakage because of SPB insertion error leads to nuclear GFP signal efflux into the cytoplasm (38). We first confirmed the efflux in the *cut12-1* ts mutant; GFP started to leak out from the nucleus 18 ± 10 min after interphase spindle disassembly at nonpermissive temperatures in 20 of 20 cells that assembled monopolar spindles [SI Appendix, Fig. S2D, 20, 30, and 70 min (38)]. In contrast, *plo1Δ* cells maintained GFP signals inside the nucleus during the early stage of mitosis, similar to the control strains (SI Appendix, Fig. S2C). These data suggest that SPBs are

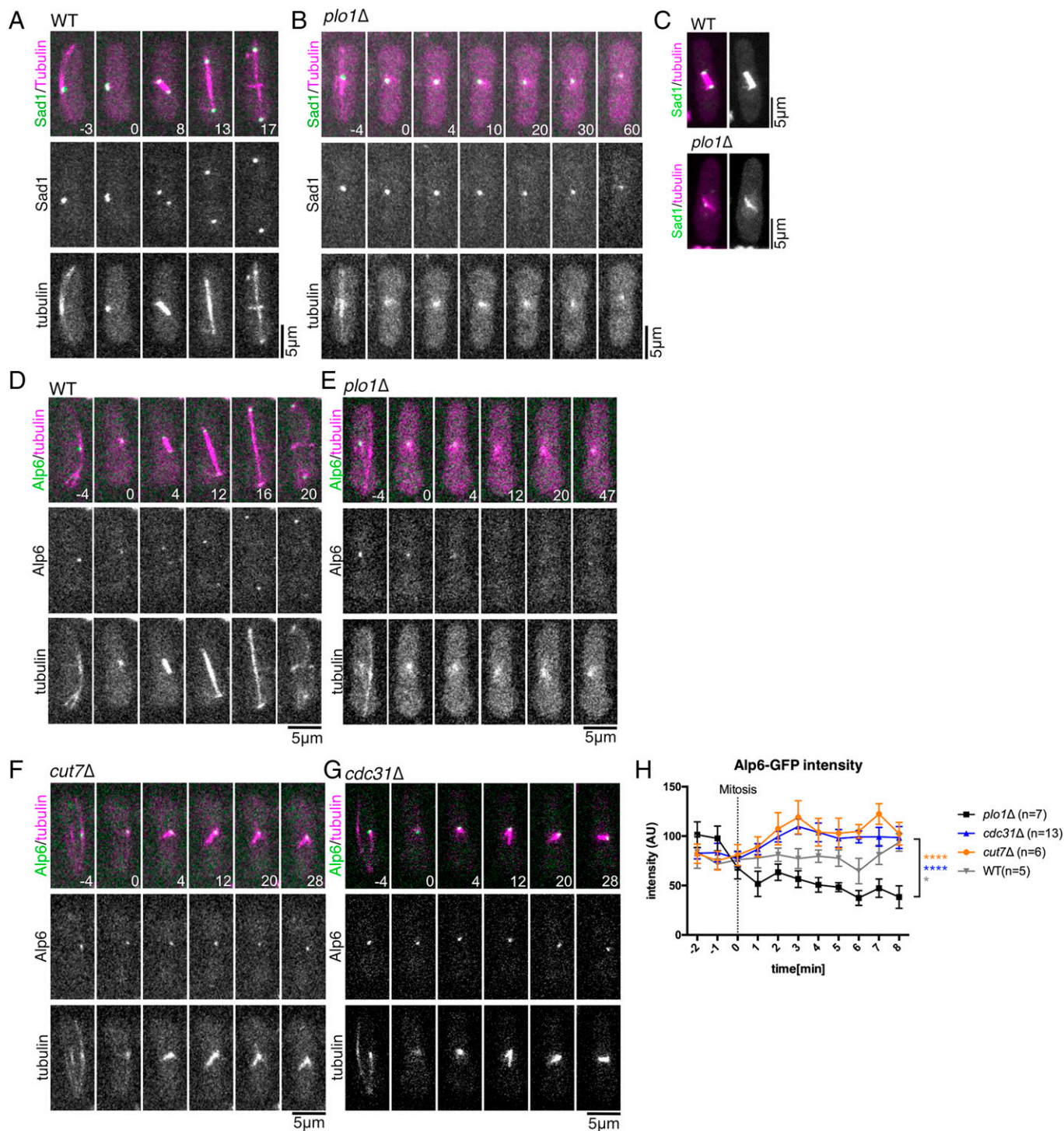


Fig. 2. Monopolar spindle formation with reduced MTs and γ -TuRC localization in *plo1Δ*. (A and B) Live imaging of the control and *plo1Δ* strains expressing Sad1^{SUN}-GFP and mCherry-tubulin. The first mitotic phase after spore germination was imaged. (C) Mitotic spindles of control and *plo1Δ* strains expressing Sad1^{SUN}-GFP and mCherry-tubulin with longer exposure time. (D and E) Live imaging of the control and *plo1Δ* strains expressing Alp6^{GCP3}-GFP and mCherry-tubulin. (F and G) Monopolar spindles of the *cut7Δ* and *cdc31Δ* strains after germination. (H) Quantification of Alp6^{GCP3}-GFP intensity during mitosis. The signal intensities from 5 to 8 min were compared between the *plo1Δ* and the wild type (WT), *cut7Δ*, or *cdc31Δ*. Error bars indicate the SEM. Time 0 (minutes) was set at the onset of spindle formation. * $P = 0.0226$; **** $P < 0.0001$. AU, arbitrary unit.

properly inserted into the NE at the onset of spindle formation in the absence of Plo1. Notably, GFP efflux during mitotic arrest occurred in 16 of 20 *plo1Δ* cells (69 ± 18 min after spindle assembly), suggesting that the integrity of NE was compromised during prolonged arrest (SI Appendix, Fig. S2C, 100 and 200 min).

Next, we isolated *cut7Δ* and *cdc31Δ* spores with Alp6^{GCP3}-GFP (SPB) and mCherry-tubulin markers and germinated

them in normal culture medium. As expected, monopolar spindles were prevalent in each sample, with only a single dot of Alp6^{GCP3}-GFP detectable at the end of spindle MTs (Fig. 2 F and G). However, Alp6^{GCP3}-GFP signal intensity was significantly lower in the *plo1Δ* spindles than in *cut7Δ* or *cdc31Δ* (Fig. 2H). Consistent with this phenotype, spindle MTs were dimmer in *plo1Δ* (compare Fig. 2E with Fig. 2 F and G), and *plo1Δ* was sensitive to thiabendazole (TBZ), an MT-destabilizing

drug (*SI Appendix, Fig. S3A*). Finally, we checked whether Cut7^{kinesin-5} localization was defective in *plo1Δ*, which would cause spindle monopolarization. Cut7^{kinesin-5}-GFP accumulation at the SPB and spindle was delayed in the absence of *plo1* (*SI Appendix, Fig. S3B*, 0 min). However, the signals gradually recovered and reached a level comparable with the early prometaphase of control cells, at which spindle bipolarity was not recovered (*SI Appendix, Fig. S3C*). Thus, it is unlikely that failure in Cut7^{kinesin-5} recruitment is the major cause of spindle monopolarization in *plo1Δ*. Rather, our data favor the model whereby decreased MT nucleation at SPB leads to spindle monopolarization in *plo1Δ*. Consistent with this notion, monopolar spindles have been observed in mutants of the γ -TuRC component (Alp4^{GCP2}) (45).

Modulation of MT Nucleation and Stability Bypassed Polo Essentiality. Two BOE strains had point mutations in *alp4^{GCP2}* and *alp6^{GCP3}*. Double *alp4-D440E plo1Δ* and *alp6-V664F plo1Δ* strains recovered colony formation ability in normal (high-glucose) medium (Fig. 1B). Thus, the essentiality of Plo1 was bypassed by a single specific mutation in the MT nucleating machinery. We also performed a spot test for single *alp6-V664F* and *alp4-D440E* mutants (Fig. 1C). *alp6-V664F* grew more slowly than the wild type, whereas no difference in colony growth was observed for *alp4-D440E*.

We investigated whether the mutation in *alp4* could restore γ -TuRC recruitment to the SPB in the absence of *plo1*. To address this, we isolated a double *alp4-D440E plo1Δ* mutant with Alp6^{GCP3}-GFP and mCherry-tubulin markers (Fig. 3A). Quantification indicated that both GFP and mCherry signals were partially but significantly restored by the *alp4-D440E* mutation (Fig. 3B and C). In 50% of the cells ($n = 46$), spindle bipolarity was recovered after a delay, and cytokinesis was completed (Fig. 3A, *Left*), whereas monopolar states were persistent for >60 min in 30% of the cells (Fig. 3B, *Right*), explaining the partial rescue of the viability by this specific mutant of *alp4*. Consistent with frequent spindle bipolarization, GFP efflux in the viable *alp4-D440E plo1Δ* and *glt5Δ plo1Δ* strains was less frequently observed than in single *plo1Δ* (19 and 21%, respectively; $n = 26$ and 48, respectively) (*SI Appendix, Fig. S2 E and F*).

Asp1^{PIP5K/Vip1} is another MT-related factor, and its mutation assisted in the growth of *plo1Δ* (Fig. 1B). Asp1^{PIP5K/Vip1} is known to have a kinase domain at the N terminus and a phosphatase domain at the C terminus, and the latter is required for MT destabilization (46). Interestingly, two mutations acquired during EVO were located at the C terminus (Fig. 1D). The mutation did not affect colony growth in the presence of Plo1 (Fig. 1C). However, time-lapse imaging showed that the *asp1-D507G plo1Δ* strain exhibited more spindle MT signals than *plo1Δ*, indicating that mutations in the C-terminal domain of Asp1 cause spindle MT stabilization (Fig. 3D–G). These data suggested that bypass of Plo1 essentiality is achieved by increasing MT stability and/or generation.

Glucose Limitation Bypasses Plo1 Essentiality. The mechanism by which glucose limitation recovers the viability of *plo1Δ* is not readily explainable. Glucose reduction did not appear to change Plo1-GFP localization. Both in high (3%) and low (0.08%) glucose media, Plo1-GFP was localized to SPBs from prophase to metaphase and delocalized at anaphase (*SI Appendix, Fig. S4 A and B*). To observe the process of mitosis, we followed Alp6^{GCP3}-GFP and spindle MTs in double *glt5Δ plo1Δ* (*Glt5* is a glucose transporter). Interestingly, Alp6^{GCP3}-GFP

accumulation at the SPB and spindle MT abundance were restored in the double mutant (Fig. 4A–D). MTs appeared to be more stable in *glt5Δ*, as incomplete disassembly of interphase MTs was often observed at the onset of mitosis, which reflected more total mCherry signals in the mutant than in the wild type (arrows in Fig. 4B). Consistent with this observation, *glt5Δ* conferred resistance to TBZ (*SI Appendix, Fig. S3D*).

Next, we tested the localization of Mid1^{anillin}, which is recruited to the equatorial region during mitosis and defines the division site, depending on phosphorylation by Plo1 (47). We observed that Mid1 was not properly localized to the cortex in the viable *glt5Δ plo1Δ* strain, whereas the cortical localization was normal in single *glt5Δ* (Fig. 4E–G). Consistent with this observation, the septum was mislocalized in *glt5Δ plo1Δ*, similar to *mid1Δ* (*SI Appendix, Fig. S4 C–E*). The results revealed that the division site positioning error was not directly linked to the lethality of *plo1Δ*. Cdc7^{Hippo} is another downstream factor of Plo1; the SPB localization of Cdc7^{Hippo} during metaphase, but not telophase, is impaired in the *plo1* mutant (48). In the viable *glt5Δ plo1Δ* strain, Cdc7^{Hippo}-GFP localization at metaphase SPB was not detectable (Fig. 4H and I). These results indicated that not all Plo1 downstream events, including the phosphorylation of the direct substrate, are restored by *glt5* mutations.

CK1 Constitutes a Masked Mechanism for Spindle Bipolarization.

Since proteins in the glucose/PKA pathway are not SPB or spindle associated, we hypothesized that other pathways are enhanced when glucose is limited, which promotes γ -TuRC localization. To identify the effector proteins in such pathways, we performed a genetic screening, with the aim to acquire mutants that were synthetic lethal with double *glt5Δ plo1Δ* or *pka1Δ plo1Δ*. For this, we first transformed a plasmid containing the *plo1⁺* gene in the double mutants, conducted mutagenesis, and selected the strains that could not lose the plasmid (Fig. 5A). A total of 13 mutants were identified that were synthetic lethal with either *glt5Δ plo1Δ* (seven strains) or *pka1Δ plo1Δ* (six strains). Possibly responsible genes were selected based on sequencing (e.g., dramatic amino acid changes, nonsense mutations, or identified in multiple strains). Synthetic lethality was confirmed for five genes (*bub1*, *hbp1*, *iml1*, *mak1*, and *wis1*) and one gene (*sin1*) by gene disruption and crossing with *glt5Δ plo1Δ* and *pka1Δ plo1Δ*, respectively. However, two mutants (*iml1* and *wis1*) and one mutant (*sin1*) resulted in poor growth when singly combined with *glt5Δ* and *pka1Δ*, respectively. These were excluded from further analysis because the major basis of synthetic lethality may not involve the lack of Plo1 kinase. *mak1* showed complex genetic interaction; while *mak1Δ glt5Δ* grew normally, synthetic lethality was revealed when mCherry-tubulin was introduced. In addition, the double *mak1Δ pka1Δ* grew poorly in the absence of mCherry-tubulin expression. Therefore, this gene was also excluded from further analyses. In contrast, triple disruption was not selected for two other genes, *bub1* and *hbp1* (*SI Appendix, Fig. S5 A and B*), whereas the double mutants with *glt5Δ* grew in a manner indistinguishable from the single *glt5Δ* even in the presence of mCherry-tubulin. We further confirmed the synthetic lethality of *hbp1Δ* with other PKA pathway genes *git1Δ plo1Δ* and *pka1Δ plo1Δ* (*SI Appendix, Fig. S5 C and D*). Thus, *bub1* and *hbp1* were essential for *plo1Δ* viability.

To identify the lethal event caused by these mutations, we observed live cells of the triple disruptants, *bub1Δ glt5Δ plo1Δ* and *hbp1Δ glt5Δ plo1Δ*. For this, we selected each triple

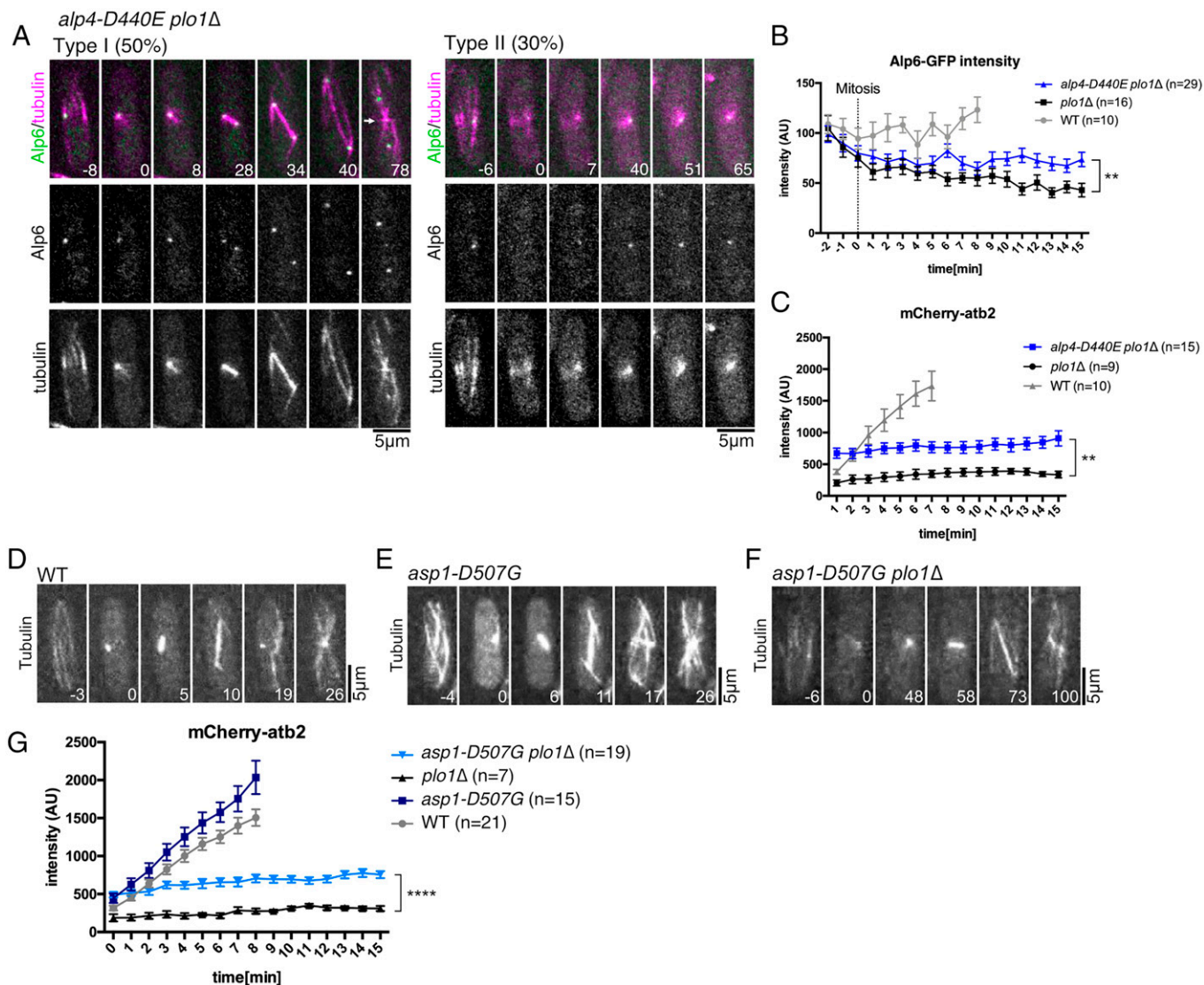


Fig. 3. MT nucleation and spindle bipolarization were rescued by a point mutation in a γ -TuRC subunit or MT destabilizer. (A, Left) Spindle bipolarization after a prolonged monopolar state by a specific mutation in the *alp4^{GCP2}* gene. Equatorial MTs during telophase were also recovered (arrow in 78 min). (A, Right) Failure in spindle bipolarization. (B and C) Partial recovery of Alp6^{GCP3}-GFP and MT intensities by a specific mutation in the *alp4^{GCP2}* gene. The signal intensities from 12 to 15 min were compared between *plo1Δ* and *alp4-D440E plo1Δ*. Alp6^{GCP3}-GFP intensity (***P* = 0.0049) and MT intensity (***P* = 0.0017). (D–G) Partial recovery of MT intensities by a mutation in the *asp1^{PIP5K/vip1}* gene. In all the graphs, error bars indicate the SEM. Time 0 (minutes) was set at the onset of spindle formation. MT intensity from 12 to 15 min was compared between *plo1Δ* with *asp1-D507G plo1Δ* (*****P* < 0.0001). WT, wild type. AU, arbitrary unit.

disruptant that possessed the Plo1-GFP multicopy plasmid. Viable cells were cultured in nonselective medium, by which cells naturally lose the plasmid at a certain probability. Time-lapse images were then acquired. We analyzed the cells that no longer had Plo1-GFP signals, as these cells represent triple gene disruptants. As a control, we prepared double *glt5Δ plo1Δ* possessing the Plo1-GFP plasmid and performed the identical “plasmid loss” culture. In the control strain that had no GFP signals, monopolar spindles were converted into bipolar spindles within 30 min, followed by entry into anaphase, in >60% cells, as expected (Fig. 5 B and E). In contrast, in triple *bub1Δ ght5Δ plo1Δ*, anaphase began even when spindles were still monopolar in 13 of 43 cells (Fig. 5C). This phenotype explains the lethality of the strain and is consistent with the fact that Bub1 is an integral component of the spindle assembly checkpoint, which prevents premature anaphase entry (49). In contrast, in *hbp1Δ ght5Δ plo1Δ*, >80% of cells were arrested in monopolar states for >30 min, and spindle bipolarization and

anaphase entry were scarcely observed, similar to the *plo1Δ* strain in the normal medium (Fig. 5 D and E). We concluded that the lethality of *hbp1Δ ght5Δ plo1Δ* comes from a defect in spindle bipolarization, similar to *plo1Δ* in the normal medium.

hbp1 encodes CK1, which is distributed throughout the cell and is enriched at the SPB (50, 51). Hhp1^{CK1} is involved in a variety of cellular processes, such as DNA repair, ubiquitination-dependent regulation of septation initiation, DNA recombination, and cohesin removal during meiosis (50, 52–54). However, to the best of our knowledge, Hhp1^{CK1} has not been directly linked to spindle function in fission yeast.

To investigate the basis of the unexpected genetic interaction, we first tested whether Hhp1^{CK1} expression/localization was altered by *ght5* disruption. To this end, we tagged GFP to Hhp1^{CK1} in the wild-type and *ght5Δ* backgrounds. Time-lapse mitosis imaging and GFP intensity quantification indicated that Hhp1^{CK1} localization was unchanged, but the overall abundance became more variable and on average, slightly increased in the

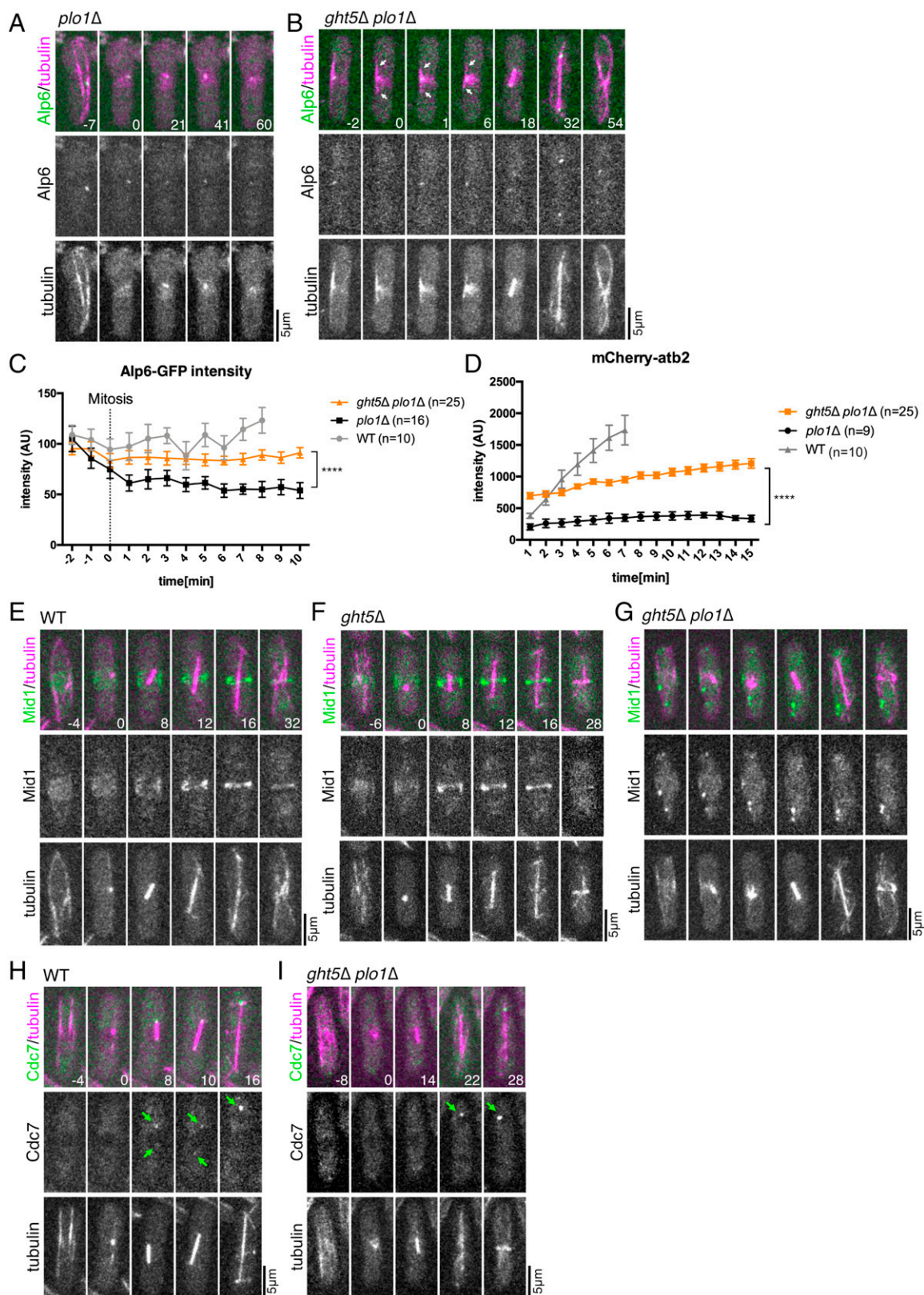


Fig. 4. γ -TuRC localization was restored by mutations in a glucose transporter in the absence of Plo1. (A) Live imaging of the *plo1Δ* strain expressing Alp6^{GFP3}-GFP and mCherry-tubulin. The first mitotic phase after spore germination was imaged. (B) Live imaging of the *ght5Δ plo1Δ* strain expressing Alp6^{GFP3}-GFP and mCherry-tubulin. Mitosis in the exponentially growing phase was imaged. Arrows indicate interphase MTs that remain during spindle assembly. (C and D) Quantification of Alp6^{GFP3}-GFP and MT intensities during mitosis. The signal intensities were compared between *plo1Δ* with *ght5Δ plo1Δ*. Error bars indicate the SEM. Control data are identical to those in Fig. 3 B and C. The increase in MT intensity during the early mitotic stage in *ght5Δ plo1Δ* is due to the incomplete disassembly of interphase MTs (arrows in B). Alp6^{GFP3}-GFP intensity from 7 to 10 min (*****P* < 0.0001) and MT intensity from 12 to 15 min (*****P* < 0.0001). (E–G) Equatorial accumulation of Mid1^{anln1}-GFP is not restored in the viable *ght5Δ plo1Δ* strain. (H and I) SPB localization of Cdc7^{Hipp0}-GFP at metaphase is not restored in the viable *ght5Δ plo1Δ* strain. Arrows indicated GFP signals at SPBs. Time 0 (minutes) was set at the onset of spindle formation. WT, wild type. AU, arbitrary unit.

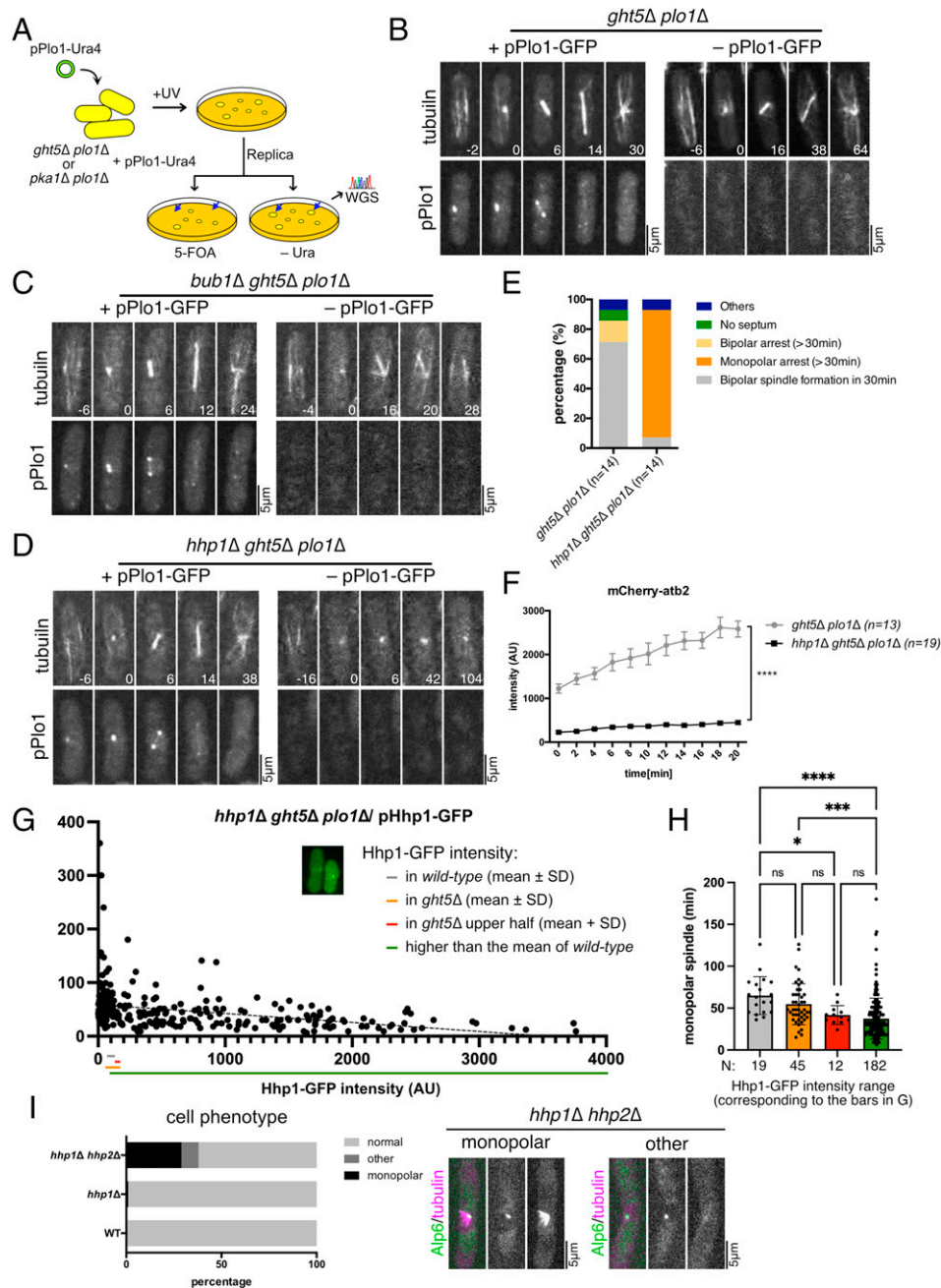


Fig. 5. Hhp1^{CK1} becomes essential for bipolar spindle formation in the absence of Plo1. (A) Schematic presentation of the synthetic lethal screening. The strain possessing Plo1 plasmid (*ura4*⁺) is sensitive to 5-fluoroorotic acid (5-FOA) and therefore, does not grow. The strain that cannot grow specifically on the 5-FOA plate should have a mutation that is synthetic lethal with *ght5Δ plo1Δ* or *pka1Δ plo1Δ*. The genome sequences of these strains were determined (WGS). (B–D) Plasmid loss experiment. The indicated double or triple disruptants transformed with Plo1-GFP plasmid were grown. Time-lapse imaging was performed, and mitotic cells with or without Plo1-GFP signals were analyzed. (E) Frequency of mitotic phenotypes (in the absence of Plo1-GFP). (F) MT intensity decreased in the absence of Hhp1^{CK1} (*****P* < 0.0001). (G) Plasmid loss experiment using *plo1Δ ght5Δ hhp1Δ* triple disruptant and multicopy Hhp1-GFP plasmid (*leu*⁺). The time spent with monopolar spindles (minutes) was plotted for each cell. GFP intensity (arbitrary units) corresponds to the amount of Hhp1 in a cell. The mean background intensity of the parental strain that had no GFP expression (80.3 AU, *n* = 31) was subtracted from the Hhp1-GFP intensity value. Mean intensities (± SD) of Hhp1-GFP signals in the wild-type background and *ght5Δ* background are indicated by gray and orange bars, respectively, whereas the red bar indicates the upper half of the values in *ght5Δ*. A simple linear regression is drawn (*R*² = 0.1202). (H) Time required for monopolar to bipolar conversion. The four colors correspond to the samples with different GFP intensities described as bars in G. Error bars represent SD. **P* = 0.0458; ****P* = 0.0001; *****P* < 0.0001. ns, *P* > 0.05. (I) A total of 29% of the *hhp1Δ hhp2Δ* cells (*n* = 79) and 1% of the *hhp1Δ* cells (*n* = 272) assembled monopolar spindles, whereas this never occurred in control cells (*n* = 336). A lack of spindle MTs was also observed in the double disruptant (Right). Time 0 (minutes) was set at the onset of spindle formation. AU, arbitrary unit.

absence of *ght5* (96 ± 23 vs. 120 ± 63 [AU, ± SD], *n* = 30 each). However, the level of *hhp1* mRNA (messenger RNA) was not elevated by a glucose reduction, suggesting that posttranscriptional regulation underlies the increased Hhp1 in the cell (SI Appendix, Fig. S5E). Next, we tested whether the up-regulation of Hhp1^{CK1} is necessary for the bypass of Plo1. We selected the

hhp1Δ ght5Δ plo1Δ triple disruptant that possesses the Hhp1^{CK1}-GFP multicopy plasmid and conducted a plasmid loss experiment. In this experiment, GFP signal intensity served as an indicator of intracellular levels of the Hhp1^{CK1} protein. Time-lapse imaging and subsequent image analysis showed that the level of the Hhp1^{CK1} protein was overall correlated with the efficiency of

spindle bipolarization (Fig. 5 *G* and *H*, gray vs. green). However, the impact of the slight increase in Hhp1^{CK1} observed in *glt5Δ* was marginal; when we compared the time required for monopolar to bipolar conversion, we observed a slight and statistically nonsignificant decrease (Fig. 5*H*, gray vs. orange). Thus, a moderate increase in Hhp1^{CK1} facilitates bipolar spindle formation in the absence of Plo1 and Ght5, although it may not be a prerequisite for BOE.

Next, we investigated whether ectopic expression of Hhp1^{CK1} was sufficient for the recovery of *plo1Δ* viability. We tested the expression of Hhp1^{CK1} by two different promoters on the multicopy plasmid, but we could not obtain data that reproducibly showed that Hhp1^{CK1} expression restored *plo1Δ* colonies (SI Appendix, Fig. S5*F*). In addition, Hhp1^{CK1} expression from the plasmid did not enhance the growth of *alp6-V664F plo1Δ* or

alp4-D440E plo1Δ, which was viable on its own but had slower growth than the wild type (SI Appendix, Fig. S5*F*). Thus, an increase in Hhp1^{CK1} levels alone did not increase the fitness of *plo1Δ* and was insufficient for the bypass of Plo1 essentiality.

Finally, we observed spindle dynamics in the *hbp1* single disruptant. Most of the cells (99%) assembled bipolar spindles, and mitosis proceeded comparably with the wild type. However, among the 272 cells monitored, we found that 3 cells (1%) formed monopolar spindles; this was not observed in our imaging of control Hhp1^{CK1+} cells (*N* > 336) (Fig. 5*I*). Furthermore, *hbp1Δ ght5Δ* was more sensitive to TBZ than *glt5Δ* (SI Appendix, Fig. S3*D*). Thus, Hhp1^{CK1} has a very mild, almost negligible level of contribution to MT stability and bipolar spindle assembly in the presence of Plo1 but becomes essential in the absence of Plo1. In *S. pombe*, *hbp2*⁺ also

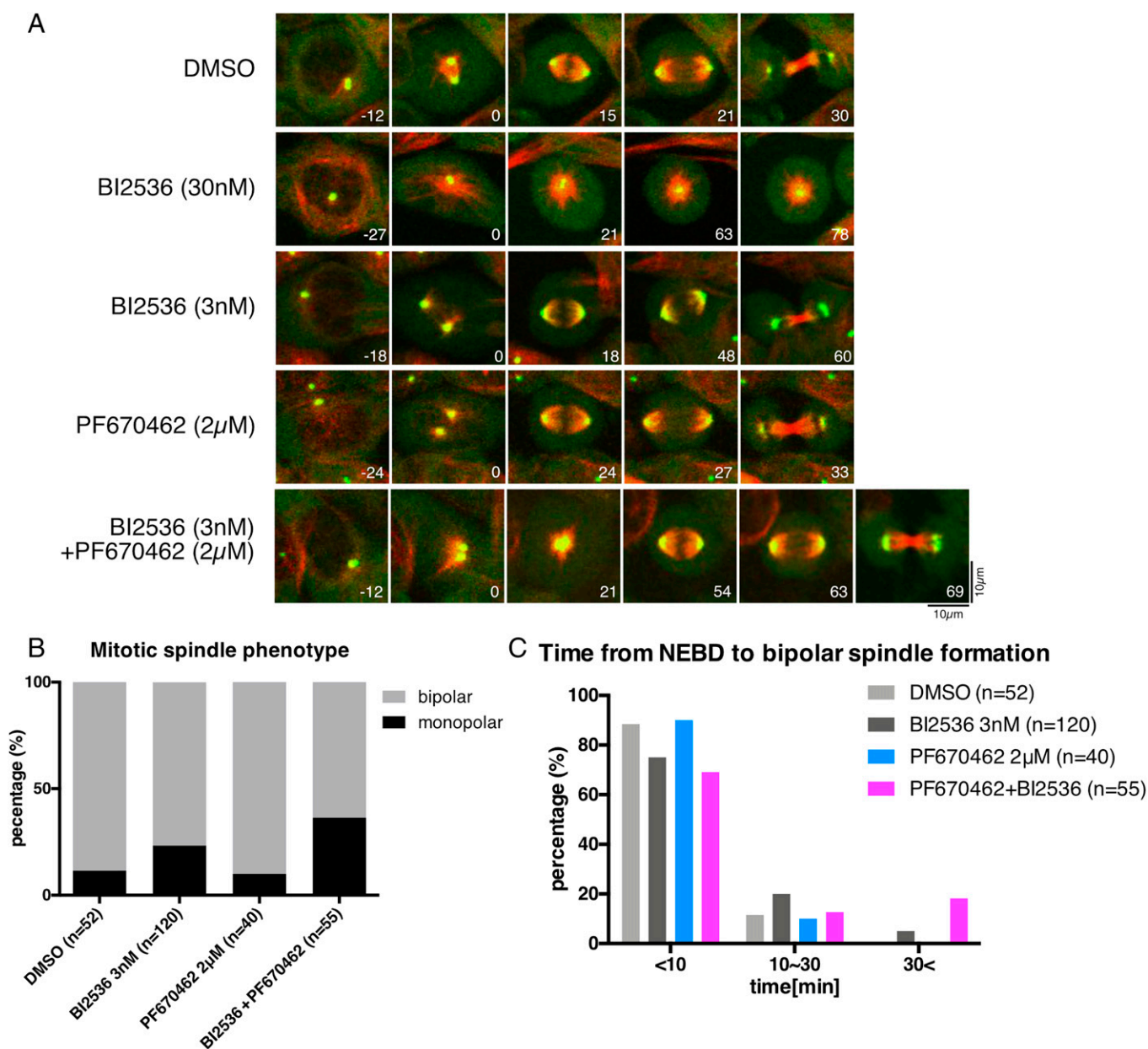


Fig. 6. Synthetic monopolar spindle phenotype by partial inhibition of Plk1 and CK1δ in human colon cancer cells. (A) Mitosis of the HCT116 cell line in the presence of Plk1 and/or CK1 inhibitors (BI2536 for Plk1, PF670462 for CK1). Green, γ -tubulin-mClover (endogenously tagged) (63); red, SiR (silicon rhodamine)-tubulin. (B) Frequency of monopolar spindles (monopolar state for ≥ 10 min). (C) Duration of nuclear envelope breakdown (NEBD) to bipolar spindle formation. Time 0 (minutes) was set at the onset of spindle formation. DMSO, dimethyl sulfoxide.

encodes CK1 (52). Therefore, we selected the *hhp1Δ hhp2Δ* double disruptant expressing mCherry-tubulin and $\text{Alp6}^{\text{GCP3-GFP}}$ and performed time-lapse microscopy. Interestingly, monopolar spindles appeared at a much higher frequency than single *hhp1Δ* (29%, $n = 79$) (Fig. 5I). Other phenotypes, such as undeveloped spindle MTs, were also observed in the double disruptant (Fig. 5I, Right). We further determined if *hhp2Δ* would be synthetically lethal with three viable *plo1Δ* strains (*ght5Δ plo1Δ*, *git1Δ plo1Δ*, and *pka1Δ plo1Δ*). Unlike *hhp1Δ*, no strains showed synthetic lethality with *hhp2Δ*. Thus, Hhp1^{CK1} and Hhp2^{CK1} were not completely redundant for bypass-related functions, which corroborates the previous report that they are different in subcellular localization and abundance (51).

Masked Contribution of CK1 to Spindle Formation in a Human Colon Cancer Cell Line. Among the four Plks in mammals, Plk1 is required for centrosome maturation and bipolar spindle formation in many cell types and is thus most analogous to *S. pombe* Plo1. There are also several CK1 family members in mammals. As CK1 δ is localized at the centrosome (55, 56), we tested whether CK1 δ constitutes the masked mechanism behind Plk1 in human cells (Fig. 6). The treatment of a human colon cancer line (HCT116) with a low concentration (3 nM) of Plk1 inhibitor BI2536 resulted in a slightly higher frequency of monopolar spindle appearance in early prometaphase (Fig. 6A and B). PF670462, an inhibitor of CK1 δ/ϵ (57, 58), did not increase the number of monopolar spindles. However, when both inhibitors were simultaneously treated, 36% of the cells first assembled monopolar spindles (Fig. 6A and B). The monopolar spindles were eventually converted to bipolar spindles; however, this process required >30 min in ~20% of the cells when two compounds were simultaneously added (Fig. 6C). These results highlight the importance of CK1, perhaps CK1 δ , in spindle bipolarization in human colon cancer cells, when Plk1 function is partially impaired.

Discussion

This study represents a rare example of the experimental BOE of genes required for mitosis. The BOE occurrence in Plo1 was unexpected, as it has been recognized as a versatile, essential kinase in mitosis not only in animal cells but also, in fission yeast. However, there is evolutionary evidence supporting that this gene can be deletable; for example, plants have lost Plks, whereas the ancestral algae possess Plks (59). In our initial BOE screening using *plo1Δ* spores, only one viable strain was recovered, in which the gene encoding the glucose transporter *Ght5* was lost through a deletion event. Subsequent evolutionary repair (EVO) experiments led to the identification of more mutations, many of which restored viability of *plo1Δ* without the *ght5* mutation. Thus, the initial mutagenesis-based screen was not sensitive enough to capture all the possible BOE. More BOE may be uncovered in the yeast system, including BOE-M, by applying more sensitive methods or simply by increasing the screen scale.

Plo1 loss can be rendered nonlethal by mutations in several genes, some of which were unrelated to each other and not associated with spindle functions at first glance. However, this is in accordance with many previous examples of BOE or evolutionary repair in the laboratory, where compensatory mutations are often found in genes outside of the perturbed functional module (3). Subsequent analysis suggested that bypass mutations converge into a common outcome: the

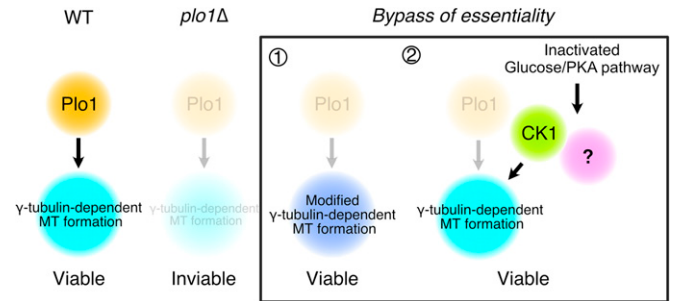


Fig. 7. How Plo1 essentiality is bypassed. An increase in spindle MTs is the key to bypassing Plo1. This can be achieved by 1) mutations in MT-associated proteins or nucleators or 2) global change in glucose metabolism, which involves CK1 and other unknown factors. WT, wild type.

increase in spindle MTs. This was achieved by multiple direct and indirect mechanisms, such as mutations in an MT destabilizer and MT nucleator, or through glucose starvation. In contrast, the septum phenotype was not rescued in a viable strain. Thus, although multiple defects have been identified in the *plo1* mutants, MT formation is directly linked to viability. In a broader sense, BOE analysis could be used to distinguish between essential and nonessential functions of an essential gene.

The bypass of Plo1 essentiality by glucose reduction in the medium is intriguing from multiple perspectives. First, it illustrates the nonabsolute nature of gene essentiality (1). If the low-glucose medium was used as the standard yeast culture medium, then Plo1 would have been assigned as a nonessential gene in *S. pombe*. Second, a change in available nutrients occurs, perhaps frequently, in the natural yeast habitat. The decrease in available glucose allows the yeast to lose a critical mitotic kinase and develop an alternative mechanism. The data support the theory that environmental change combined with gene mutations drives molecular diversity, namely variation in genes required for an essential process (3). Third, the change in fundamental metabolism alters the expression of many genes (60), offering a unique “genetic background” that is not achieved by mutations in a few mitotic genes. In the case of *plo1Δ*, a critical factor for survival was Hhp1^{CK1} . Because Hhp1^{CK1} is SPB associated, it is possible that critical Plo1 substrates (such as γ -TuRC or its associated factor) are phosphorylated by Hhp1^{CK1} . However, CK1 is unlikely the sole element of BOE based on glucose repression, and other factors should be also involved, as Hhp1^{CK1} overexpression alone was not sufficient to restore the viability of *plo1Δ* (Fig. 7). Interestingly, *Saccharomyces cerevisiae* $\text{Hrr25}^{\text{CK1}}$ can phosphorylate and activate the γ -tubulin complex in vitro, and this phosphorylation is required for in vivo γ -tubulin functions (61). Whether $\text{Hrr25}^{\text{CK1}}$ constitutes a masked mechanism of $\text{Cdc5}^{\text{Plk1}}$ in *S. cerevisiae* is an intriguing question for future investigation.

BOE, or synthetic viability, is a critical challenge in cancer chemotherapy because of the emergence of resistance (62). Plk inhibitors have been recognized as promising antitumor drugs (21, 23). However, our study suggests that there may be resistant cells involving CK1 and that double inhibition of Plk1 and CK1 δ may be more suitable for mitotic cell perturbation.

Materials and Methods

Materials and methods on yeast and human cell culture, strain selection, live microscopy, genetic screening and confirmation, EVO, WGS, real-time PCR, and statistics are described in *SI Appendix, Materials and Methods*.

Data Availability. All study data are included in the article and/or supporting information.

ACKNOWLEDGMENTS. We thank Aoi Takeda for help with the EVO culture; Shigeaki Saitoh (Kurume University), Kojiro Takeda (Konan University), Masamitsu Sato (Waseda University), Iain Hagan (University of Manchester), Ye Dee Tay (University of Edinburgh), and the National Bio-Resource Project of the Ministry of Education, Culture, Sports, Science and Technology, Japan for yeast strains and plasmids; Kazuma Uesaka for help with sequence analysis; Ken

Sawin, Hiro Ohkura, and Ye Dee Tay (University of Edinburgh) for valuable discussions and protocols; Rie Inaba, Kyoko Zenbutsu, and Miki Ueda for media preparation; and Shigeaki Saitoh and Moé Yamada for comments on the manuscript. This work was supported by the Nagoya University Research Fund associated with Japan Science and Technology Agency (JST) SPRING (J.K.), Japan Society for the Promotion of Science (JSPS) KAKENHI Grants 17H01431 (to G.G.) and 19K22383 (to G.G.), JSPS Joint Research Projects with UK Research and Innovation (G.G.), and Uehara Memorial Foundation Grant 202120392 (to G.G.).

1. G. Rancati, J. Moffat, A. Typas, N. Pavelka, Emerging and evolving concepts in gene essentiality. *Nat. Rev. Genet.* **19**, 34–49 (2018).
2. C. J. Ryan, N. J. Krogan, P. Cunningham, G. Cagney, All or nothing: Protein complexes flip essentiality between distantly related eukaryotes. *Genome Biol. Evol.* **5**, 1049–1059 (2013).
3. T. LaBar, Y. Y. Phoebe Hsieh, M. Fumasoni, A. W. Murray, Evolutionary repair experiments as a window to the molecular diversity of life. *Curr. Biol.* **30**, R565–R574 (2020).
4. J. van Leeuwen *et al.*, Systematic analysis of bypass suppression of essential genes. *Mol. Syst. Biol.* **16**, e9828 (2020).
5. G. Liu *et al.*, Gene essentiality is a quantitative property linked to cellular evolvability. *Cell* **163**, 1388–1399 (2015).
6. J. Li *et al.*, Systematic analysis reveals the prevalence and principles of bypassable gene essentiality. *Nat. Commun.* **10**, 1002 (2019).
7. A. Takeda, S. Saitoh, H. Ohkura, K. E. Sawin, G. Goshima, Identification of 15 new bypassable essential genes of fission yeast. *Cell Struct. Funct.* **44**, 113–119 (2019).
8. B. Sønnichsen *et al.*, Full-genome RNAi profiling of early embryogenesis in *Caenorhabditis elegans*. *Nature* **434**, 462–469 (2005).
9. B. Neumann *et al.*, Phenotypic profiling of the human genome by time-lapse microscopy reveals cell division genes. *Nature* **464**, 721–727 (2010).
10. K. L. McKinley, I. M. Cheeseman, Large-scale analysis of CRISPR/Cas9 cell-cycle knockouts reveals the diversity of p53-dependent responses to cell-cycle defects. *Dev. Cell* **40**, 405–420.e2 (2017).
11. P. T. Conduit, A. Wainman, J. W. Raff, Centrosome function and assembly in animal cells. *Nat. Rev. Mol. Cell Biol.* **16**, 611–624 (2015).
12. M. Yamada, G. Goshima, Mitotic spindle assembly in land plants: Molecules and mechanisms. *Biology (Basel)* **6**, E6 (2017).
13. S. Gourguechon, L. J. Holt, W. Z. Cande, The Giardia cell cycle progresses independently of the anaphase-promoting complex. *J. Cell Sci.* **126**, 2246–2255 (2013).
14. R. D. Vale, The molecular motor toolbox for intracellular transport. *Cell* **112**, 467–480 (2003).
15. S. Y. Leong, T. Edzuka, G. Goshima, M. Yamada, Kinesin-13 and Kinesin-8 Function during cell growth and division in the moss *Physcomitrella patens*. *Plant Cell* **32**, 683–702 (2020).
16. M. Hara, M. Ariyoshi, E. I. Okumura, T. Hori, T. Fukagawa, Multiple phosphorylations control recruitment of the KMN network onto kinetochores. *Nat. Cell Biol.* **20**, 1378–1388 (2018).
17. F. Malvezzi *et al.*, A structural basis for kinetochore recruitment of the Ndc80 complex via two distinct centromere receptors. *EMBO J.* **32**, 409–423 (2013).
18. M. Yukawa, C. Ikebe, T. Toda, The Msd1-Wdr8-Pkl1 complex anchors microtubule minus ends to fission yeast spindle pole bodies. *J. Cell Biol.* **209**, 549–562 (2015).
19. V. Syrovatkina, P. T. Tran, Loss of kinesin-14 results in aneuploidy via kinesin-5-dependent microtubule protrusions leading to chromosome cut. *Nat. Commun.* **6**, 7322 (2015).
20. Z. T. Olmsted, A. G. Colliver, T. D. Riehlman, J. L. Paluh, Kinesin-14 and kinesin-5 antagonistically regulate microtubule nucleation by γ -TuRC in yeast and human cells. *Nat. Commun.* **5**, 5339 (2014).
21. T. Otto, P. Sicinski, Cell cycle proteins as promising targets in cancer therapy. *Nat. Rev. Cancer* **17**, 93–115 (2017).
22. V. Archambault, D. M. Glover, Polo-like kinases: Conservation and divergence in their functions and regulation. *Nat. Rev. Mol. Cell Biol.* **10**, 265–275 (2009).
23. C. E. Cunningham *et al.*, The CINs of polo-like kinase 1 in cancer. *Cancers (Basel)* **12**, E2953 (2020).
24. S. Saitoh *et al.*, Mechanisms of expression and translocation of major fission yeast glucose transporters regulated by CaMKK/phosphatases, nuclear shuttling, and TOR. *Mol. Biol. Cell* **26**, 373–386 (2015).
25. P. A. Grant, F. Winston, S. L. Berger, The biochemical and genetic discovery of the SAGA complex. *Biochim. Biophys. Acta. Gene Regul. Mech.* **1864**, 194669 (2021).
26. S. M. Byrne, C. S. Hoffman, Six git genes encode a glucose-induced adenylate cyclase activation pathway in the fission yeast *Schizosaccharomyces pombe*. *J. Cell Sci.* **105**, 1095–1100 (1993).
27. T. Maeda, Y. Watanabe, H. Kunitomo, M. Yamamoto, Cloning of the pka1 gene encoding the catalytic subunit of the cAMP-dependent protein kinase in *Schizosaccharomyces pombe*. *J. Biol. Chem.* **269**, 9632–9637 (1994).
28. S. Shashkova, N. Welkenhuysen, S. Hohmann, Molecular communication: Crosstalk between the Snf1 and other signaling pathways. *FEMS Yeast Res.* **15**, fov026 (2015).
29. A. Klip, T. Tsakiridis, A. Marette, P. A. Ortiz, Regulation of expression of glucose transporters by glucose: A review of studies in vivo and in cell cultures. *FASEB J.* **8**, 43–53 (1994).
30. M. Kelkar, S. G. Martin, PKA antagonizes CLASP-dependent microtubule stabilization to re-localize Pom1 and buffer cell size upon glucose limitation. *Nat. Commun.* **6**, 8445 (2015).
31. P. Liu, M. Würtz, E. Zupa, S. Pfeiffer, E. Schiebel, Microtubule nucleation: The waltz between γ -tubulin ring complex and associated proteins. *Curr. Opin. Cell Biol.* **68**, 124–131 (2021).
32. P. Lénárt *et al.*, The small-molecule inhibitor BI 2536 reveals novel insights into mitotic roles of polo-like kinase 1. *Curr. Biol.* **17**, 304–315 (2007).
33. K. Tanaka *et al.*, The role of Plo1 kinase in mitotic commitment and septation in *Schizosaccharomyces pombe*. *EMBO J.* **20**, 1259–1270 (2001).
34. J. Bähler *et al.*, Role of polo kinase and Mid1p in determining the site of cell division in fission yeast. *J. Cell Biol.* **143**, 1603–1616 (1998).
35. S. Wälde, M. C. King, The KASH protein Kms2 coordinates mitotic remodeling of the spindle pole body. *J. Cell Sci.* **127**, 3625–3640 (2014).
36. H. Ohkura, I. M. Hagan, D. M. Glover, The conserved *Schizosaccharomyces pombe* kinase plo1, required to form a bipolar spindle, the actin ring, and septum, can drive septum formation in G1 and G2 cells. *Genes Dev.* **9**, 1059–1073 (1995).
37. A. Gallert *et al.*, Centrosomal MPF triggers the mitotic and morphogenetic switches of fission yeast. *Nat. Cell Biol.* **15**, 88–95 (2013).
38. V. A. Tallada, K. Tanaka, M. Yanagida, I. M. Hagan, The *S. pombe* mitotic regulator Cut12 promotes spindle pole body activation and integration into the nuclear envelope. *J. Cell Biol.* **185**, 875–888 (2009).
39. A. J. Bridge, M. Morphew, R. Bartlett, I. M. Hagan, The fission yeast SPB component Cut12 links bipolar spindle formation to mitotic control. *Genes Dev.* **12**, 927–942 (1998).
40. I. Hagan, M. Yanagida, Novel potential mitotic motor protein encoded by the fission yeast cut7+ gene. *Nature* **347**, 563–566 (1990).
41. A. Paoletti *et al.*, Fission yeast cdc31p is a component of the half-bridge and controls SPB duplication. *Mol. Biol. Cell* **14**, 2793–2808 (2003).
42. R. West, E. V. Vaisberg, R. Ding, P. Nurse, J. R. McIntosh, cut11(+): A gene required for cell cycle-dependent spindle pole body anchoring in the nuclear envelope and bipolar spindle formation in *Schizosaccharomyces pombe*. *Mol. Biol. Cell* **9**, 2839–2855 (1998).
43. A. J. Bestul, Z. Yu, J. R. Unruh, S. L. Jaspersen, Redistribution of centrosomal proteins by centromeres and Polo kinase controls partial nuclear envelope breakdown in fission yeast. *Mol. Biol. Cell* **32**, 1487–1500 (2021).
44. M. R. Flory, M. Morphew, J. D. Joseph, A. R. Means, T. N. Davis, Pcp1p, an Spc110p-related calmodulin target at the centrosome of the fission yeast *Schizosaccharomyces pombe*. *Cell Growth Differ.* **13**, 47–58 (2002).
45. L. Vardy, T. Toda, The fission yeast gamma-tubulin complex is required in G(1) phase and is a component of the spindle assembly checkpoint. *EMBO J.* **19**, 6098–6111 (2000).
46. J. Pöhlmann *et al.*, The Vip1 inositol polyphosphate kinase family regulates polarized growth and modulates the microtubule cytoskeleton in fungi. *PLoS Genet.* **10**, e1004586 (2014).
47. M. Almonacid *et al.*, Temporal control of contractile ring assembly by Plo1 regulation of myosin II recruitment by Mid1/anillin. *Curr. Biol.* **21**, 473–479 (2011).
48. P. Wachowicz *et al.*, Analysis of *S. pombe* SIN protein association to the SPB reveals two genetically separable states of the SIN. *J. Cell Sci.* **128**, 741–754 (2015).
49. P. Bernard, K. Hardwick, J. P. Javerzat, Fission yeast bub1 is a mitotic centromere protein essential for the spindle checkpoint and the preservation of correct ploidy through mitosis. *J. Cell Biol.* **143**, 1775–1787 (1998).
50. A. E. Johnson, J. S. Chen, K. L. Gould, CK1 is required for a mitotic checkpoint that delays cytokinesis. *Curr. Biol.* **23**, 1920–1926 (2013).
51. Z. C. Elmore, R. X. Guillen, K. L. Gould, The kinase domain of CK1 enzymes contains the localization cue essential for compartmentalized signaling at the spindle pole. *Mol. Biol. Cell* **29**, 1664–1674 (2018).
52. N. Dhillon, M. F. Hoekstra, Characterization of two protein kinases from *Schizosaccharomyces pombe* involved in the regulation of DNA repair. *EMBO J.* **13**, 2777–2788 (1994).
53. N. Phadnis *et al.*, Casein Kinase 1 and phosphorylation of cohesin subunit Rec11 (SA3) promote meiotic recombination through linear element formation. *PLoS Genet.* **11**, e1005225 (2015).
54. C. Rumpf *et al.*, Casein kinase 1 is required for efficient removal of Rec8 during meiosis I. *Cell Cycle* **9**, 2657–2662 (2010).
55. Y. E. Greer, J. S. Rubin, Casein kinase 1 delta functions at the centrosome to mediate Wnt-3a-dependent neurite outgrowth. *J. Cell Biol.* **192**, 993–1004 (2011).
56. Y. E. Greer *et al.*, Casein kinase 1 δ functions at the centrosome and Golgi to promote ciliogenesis. *Mol. Biol. Cell* **25**, 1629–1640 (2014).
57. C. Aquino Perez, M. Burocziava, G. Jenikova, L. Macurek, CK1-mediated phosphorylation of FAM110A promotes its interaction with mitotic spindle and controls chromosomal alignment. *EMBO Rep.* **22**, e51847 (2021).
58. Q. J. Meng *et al.*, Entrainment of disrupted circadian behavior through inhibition of casein kinase 1 (CK1) enzymes. *Proc. Natl. Acad. Sci. U.S.A.* **107**, 15240–15245 (2010).
59. E. Okamura, T. Sakamoto, T. Sasaki, S. Matsunaga, A plant ancestral polo-like kinase sheds light on the mystery of the evolutionary disappearance of polo-like kinases in the plant kingdom. *Cytologia (Tokyo)* **82**, 261–266 (2017).
60. S. Saitoh, M. Yanagida, Does a shift to limited glucose activate checkpoint control in fission yeast? *FEBS Lett.* **588**, 2373–2378 (2014).
61. Y. Peng *et al.*, Interaction of CK1 δ with γ TuSC ensures proper microtubule assembly and spindle positioning. *Mol. Biol. Cell* **26**, 2505–2518 (2015).
62. A. Ashworth, C. J. Lord, J. S. Reis-Filho, Genetic interactions in cancer progression and treatment. *Cell* **145**, 30–38 (2011).
63. K. Tsuchiya, G. Goshima, Microtubule-associated proteins promote microtubule generation in the absence of γ -tubulin in human colon cancer cells. *J. Cell Biol.* **220**, e202104114 (2021).